
FRACTIONAL-STEP RUNGE–KUTTA METHODS: REPRESENTATION AND LINEAR STABILITY ANALYSIS *

PREPRINT SUBMITTED TO JOURNAL OF COMPUTATIONAL PHYSICS , APRIL 13TH, 2022

Raymond J. Spiteri

Department of Computer Science
University of Saskatchewan, Saskatoon, SK, Canada

spiteri@cs.usask.ca

Siqi Wei

Department of Mathematics and Statistics
University of Saskatchewan, Saskatoon, SK, Canada

siqi.wei@usask.ca

ABSTRACT

Fractional-step methods are a popular and powerful divide-and-conquer approach for the numerical solution of differential equations. When the integrators of the fractional steps are Runge–Kutta methods, such methods can be written as generalized additive Runge–Kutta (GARK) methods, and thus the representation and analysis of such methods can be done through the GARK framework. We show how the general Butcher tableau representation and linear stability of such methods are related to the coefficients of the splitting method, the individual sub-integrators, and the order in which they are applied. We use this framework to explain some observations in the literature about fractional-step methods such as the choice of sub-integrators, the order in which they are applied, and the role played by negative splitting coefficients in the stability of the method.

Keywords operator-splitting, fractional-step methods, implicit-explicit methods, generalized-structure additive Runge–Kutta methods, linear stability analysis

1 Introduction

The right-hand side of an explicit ordinary differential equation (ODE) is often additively comprised of terms having different character, e.g., linear vs. nonlinear, stiff vs. non-stiff, or derived from different physical phenomena such as advection vs. reaction vs. diffusion. In such cases, it is natural (and often advantageous) to consider a splitting approach that treats the different terms with different numerical methods. In this way, the terms can be treated in specialized ways, potentially leading to efficient methods or ones with special properties such as symplecticity or strong stability. Indeed, when using different libraries as black boxes for simulations of different parts of the system as in co-simulation (see, e.g., Gomes et al. [2018] and references therein), there may be no choice but treat the parts separately. Similarly, it may not be feasible to solve certain problems in a monolithic sense.

Divide-and-conquer approaches to solving ODEs date at least as far back as Sophus Lie in the 1870s Lie and Engel [1970]. They have a long and diverse history, and because of this, they have been known by many names and have subtle differences between them. Such names include operator splitting, time splitting, split-step methods, dimensional splitting, locally one-dimensional (LOD) methods, alternating direction implicit (ADI) methods, approximate matrix factorization (AMF) methods, and additive methods (and their most popular special case, implicit-explicit (IMEX) methods); see, e.g., Hundsdorfer and Verwer [2003], McLachlan and Quispel [2002], Glowinski et al. [2017] and references therein. When used to solve differential-algebraic equations, such as those arising from the incompressible Navier–Stokes equations, they are also called projection methods; see, e.g., Guermond et al. [2006] and references therein.

*This work was supported by the National Sciences and Engineering Research Council of Canada through its Discovery Grant program.

Consider the initial-value problem (IVP) for an N -additively split ordinary differential equation

$$\frac{dy}{dt} = \mathcal{F}(t, y) = \sum_{\ell=1}^N \mathcal{F}^{[\ell]}(t, y), \quad y(0) = y_0. \quad (1)$$

In this study, we focus on *fractional-step methods*, as termed by Yanenko [1971], whereby the various terms $\mathcal{F}^{[\ell]}$ of the right-hand side of the ODE are integrated in turn. The output from a given sub-integration is used as input to the next one. An approximation to the solution $y(t)$ is eventually produced when all the terms have been appropriately integrated.

Fractional-step methods are based on two fundamental parts: the (operator) splitting method and the sub-integrators. The simplest and most well-known examples of operator-splitting methods for ODEs include the Lie–Trotter Trotter [1958] or Godunov Godunov [1959] splitting method and the Strang–Marchuk splitting method Strang [1968], Marchuk [1971]. These are low-order methods (first and second order, respectively). Symmetrized methods, whereby one splitting method is applied in tandem with its adjoint, are a popular approach for achieving higher-order splitting methods; the Strang–Marchuk splitting method can be derived from the Lie–Trotter/Godunov method in this fashion McLachlan and Quispel [2002]. The sub-integrators can range anywhere from an exact sub-flow to a standard numerical method such as linear multistep or Runge–Kutta. The classical order of the overall fractional-step method is then generally the minimum of the order of the splitting method and all the sub-integrators. The class of multi-rate methods uses sub-stepping, perhaps in an adaptive fashion using a separate integrator library like SUNDIALS or MATLAB’s `ode15s`, to perform the sub-integrations to within a specified error tolerance Ropp et al. [2004].

When Runge–Kutta methods are used as the sub-integrators for each fractional step, the result is a fractional step Runge–Kutta (FSRK) method that can be cast in the framework of a generalized-structure additive Runge–Kutta (GARK) method. Such representations have appeared to various degrees of generality, e.g., Christlieb et al. [2015], González-Pinto et al. [2022]. Here, we show how to systematically construct the Butcher tableau representation of a general FSRK method, i.e., one having an arbitrary Runge–Kutta method as sub-integrator at each of s splitting stages and N operators.

Linear stability is an important property of a numerical method. It is generally an important indicator in the design and performance of a numerical method in practice. In this paper, we use the Butcher tableau representation of GARK methods to study the linear stability of FSRK methods, give an interpretation of the stability function in terms of the splitting method coefficients and the individual Runge–Kutta methods, and show how the linear stability theory presented to explain common observations in previously published studies on the stability behavior of fractional-step methods.

Before proceeding further, it should be noted that it is widely accepted that no single numerical method is a silver bullet that will outperform all other methods on all problems. Fractional-step methods are no exception. Well-known issues with the use of splitting methods in general include the specification of boundary conditions Hundsdorfer and Verwer [2003] as well as convergence to spurious steady states Speth et al. [2013], Glowinski et al. [2017]. A significant body of literature exists to address these and other issues surrounding the implementation of operator-splitting methods in practice, but a full discussion is beyond the scope of this study.

The remainder of the paper is organized as follows. The necessary definitions and theoretical background on operator-splitting, GARK, and FSRK methods are given in section 2. The main theoretical results on the Butcher tableau representation and linear stability of FSRK methods appear in section 3. Some examples on the use of these theoretical results are provided in section 4. The examples illustrate how observations in the literature can be explained in the general framework set out in this paper. Conclusions follow in section 5.

2 Background

In this section, we present some necessary background to construct FSRK methods, including the definition of operator-splitting methods, additive Runge–Kutta (ARK) methods as introduced in Cooper and Sayfy [1980], and their evolution to GARK methods presented in Sandu and Günther [2015].

2.1 Operator-splitting methods

We begin by presenting operator-splitting methods as discussed in Hairer et al. [2006]. Let $\varphi_{\Delta t}^{[\ell]}$ be the flow of the subsystem $\frac{dy^{[\ell]}}{dt} = \mathcal{F}^{[\ell]}(t, y^{[\ell]})$ for $\ell = 1, 2, \dots, N$. Compositions of $\varphi_{\Delta t}^{[\ell]}$ for $\ell = 1, 2, \dots, N$, such as

$$\Phi_{\Delta t} := \varphi_{\Delta t}^{[N]} \circ \varphi_{\Delta t}^{[N-1]} \circ \dots \circ \varphi_{\Delta t}^{[1]}, \quad (2a)$$

$$\Phi_{\Delta t}^* := \varphi_{\Delta t}^{[1]} \circ \varphi_{\Delta t}^{[2]} \circ \dots \circ \varphi_{\Delta t}^{[N]} \quad (2b)$$

are two numerical methods to solve eq. (1). The two methods eq. (2a) and (2b) are adjoints of each other and are both first-order accurate. In particular, eq. (2a) is known as the Lie–Trotter (or Godunov) splitting method, although the same name could apply to (2b) by a re-numbering of the operators. The second-order Strang–Marchuk splitting method can be viewed a composition of the Lie–Trotter method and its adjoint with halved step sizes and can be written as

$$\begin{aligned} \Psi_{\Delta t}^S &= \Phi_{\Delta t/2}^* \circ \Phi_{\Delta t/2} \\ &= \varphi_{\Delta t/2}^{[1]} \circ \varphi_{\Delta t/2}^{[2]} \circ \dots \circ \varphi_{\Delta t/2}^{[N-1]} \circ \varphi_{\Delta t}^{[N]} \circ \varphi_{\Delta t/2}^{[N-1]} \circ \dots \circ \varphi_{\Delta t/2}^{[1]}. \end{aligned}$$

Remark 1. We note that the term $\varphi_{\Delta t}^{[N]}$ arises from the group property of exact flows. This term is often approximated directly. However, it is possible to approximate the two occurrences $\varphi_{\Delta t/2}^{[N]}$ separately, leading to a *different numerical method (with different accuracy and stability properties)*.

The general form of the operator-splitting method considered in this paper is expressed as follows. Let $\alpha = \{\alpha_1, \alpha_2, \dots, \alpha_s\}$, where $\alpha_k = \{\alpha_k^{[1]}, \alpha_k^{[2]}, \dots, \alpha_k^{[N]}\}$, $k = 1, 2, \dots, s$, be the coefficients of the splitting method. An s -stage operator-splitting method that solves (1) can be written as

$$\Psi_{\Delta t} := \prod_{k=1}^s \Phi_{\alpha_k \Delta t}^{\{k\}} = \Phi_{\alpha_s \Delta t}^{\{s\}} \circ \Phi_{\alpha_{s-1} \Delta t}^{\{s-1\}} \circ \dots \circ \Phi_{\alpha_1 \Delta t}^{\{1\}}, \quad (3)$$

where $\Phi_{\alpha_k \Delta t}^{\{k\}} := \varphi_{\alpha_k^{[N]} \Delta t}^{[N]} \circ \varphi_{\alpha_k^{[N-1]} \Delta t}^{[N-1]} \circ \dots \circ \varphi_{\alpha_k^{[1]} \Delta t}^{[1]}$. The operator-splitting method eq. (3) can be viewed as a general additive method but where only specific coupling between the operators is allowed (see below). Hence, the accuracy and stability properties can be expected to be inferior to additive methods. Additive methods, however, are not applicable for co-simulations where the simulations of subsystems must be treated as black boxes and data between subsystems can only be exchanged after a subsystem is integrated. Hence, the study of operator-splitting methods of the form eq. (3) have a broad range of application despite their rather specific nature.

2.2 RK and ARK methods

Definition 2.1. (Runge–Kutta method) Let b_i and a_{ij} , $i, j = 1, 2, \dots, \tilde{s}$, be real numbers, and let $c_i = \sum_{j=1}^{\tilde{s}} a_{ij}$. One step of an \tilde{s} -stage Runge–Kutta method is given by

$$\mathbf{y}_{n+1} = \mathbf{y}_n + \Delta t \sum_{i=1}^{\tilde{s}} b_i \mathcal{F}(t_n + c_i \Delta t, \mathbf{Y}_i), \quad (4a)$$

$$\mathbf{Y}_i = \mathbf{y}_n + \Delta t \sum_{j=1}^{\tilde{s}} a_{ij} \mathcal{F}(t_n + c_j \Delta t, \mathbf{Y}_j), \quad i = 1, 2, \dots, \tilde{s}. \quad (4b)$$

The coefficients b_i , c_i , and a_{ij} , $i, j = 1, 2, \dots, \tilde{s}$, of a Runge–Kutta method can be represented as the Butcher tableau

$$\begin{array}{c|cccc} c_1 & a_{11} & a_{12} & \dots & a_{1\tilde{s}} \\ c_2 & a_{21} & a_{22} & \dots & a_{2\tilde{s}} \\ \vdots & \vdots & \vdots & \ddots & \vdots \\ c_{\tilde{s}} & a_{\tilde{s}1} & a_{\tilde{s}2} & \dots & a_{\tilde{s}\tilde{s}} \\ \hline & b_1 & b_2 & \dots & b_{\tilde{s}} \end{array} = \frac{\mathbf{c}}{\mathbf{b}} \mid \mathbf{A}.$$

For notational simplicity, we denote the quadrature weights of the Butcher tableau by \mathbf{b} rather than \mathbf{b}^T .

When different \tilde{s} -stage Runge–Kutta integrators are applied to each operator $\mathcal{F}^{[\ell]}$ of eq. (1), the numerical method is called an additive Runge–Kutta method Cooper and Sayfy [1980], Kennedy and Carpenter [2003].

Definition 2.2 (Additive Runge–Kutta method). Let $b_i^{[\ell]}, a_{ij}^{[\ell]}, i, j = 1, 2, \dots, \tilde{s}, \ell = 1, 2, \dots, N$, be real numbers, and let $c_j^{[\ell]} = \sum_{i=1}^{\tilde{s}} a_{ij}^{[\ell]}$. One step of an \tilde{s} -stage ARK method is given by

$$\mathbf{y}_{n+1} = \mathbf{y}_n + \Delta t \sum_{\ell=1}^N \sum_{i=1}^{\tilde{s}} b_i^{[\ell]} \mathcal{F}^{[\ell]}(t_n + c_i^{[\ell]} \Delta t, \mathbf{Y}_i),$$

$$\mathbf{Y}_i = \mathbf{y}_n + \Delta t \sum_{\ell=1}^N \sum_{j=1}^{\tilde{s}} a_{ij}^{[\ell]} \mathcal{F}^{[\ell]}(t_n + c_j^{[\ell]} \Delta t, \mathbf{Y}_j), \quad i = 1, 2, \dots, \tilde{s},$$

where $b_i^{[\ell]}, c_j^{[\ell]}$, and $a_{ij}^{[\ell]}$ are the coefficients of the method applied to operator $\mathcal{F}^{[\ell]}$.

The Butcher tableau for ARK methods can be written as Sandu and Günther [2015]

$$\begin{array}{c|c|c|c|c|c|c|c} \mathbf{c}^{[1]} & \mathbf{c}^{[2]} & \dots & \mathbf{c}^{[N]} & \mathbf{A}^{[1]} & \mathbf{A}^{[2]} & \dots & \mathbf{A}^{[N]} \\ \hline & & & & \mathbf{b}^{[1]} & \mathbf{b}^{[2]} & \dots & \mathbf{b}^{[N]} \end{array}, \quad (6)$$

where $\mathbf{A}^{[\ell]}, \mathbf{b}^{[\ell]}, \mathbf{c}^{[\ell]}, \ell = 1, 2, \dots, N$, are the coefficients of the Runge–Kutta method associated with operator ℓ .

2.3 GARK methods

In Sandu and Günther [2015], ARK methods were expanded to the family of generalized additive Runge–Kutta (GARK) methods, which are defined as follows:

Definition 2.3 (GARK method). Let $b_j^{[\ell]}$ and $a_{ij}^{[\ell',\ell]}, i = 1, 2, \dots, \tilde{s}^{[\ell']}, j = 1, 2, \dots, \tilde{s}^{[\ell]}, \ell' = 1, 2, \dots, N', \ell = 1, 2, \dots, N$, be real numbers, and let $c_i^{[\ell',\ell]} = \sum_{j=1}^{\tilde{s}^{[\ell]}} a_{ij}^{[\ell',\ell]}$. One step of a GARK method with an N -way additive splitting of the right-hand side of (1) with N' stages reads

$$\mathbf{y}_{n+1} = \mathbf{y}_n + \Delta t \sum_{\ell=1}^N \sum_{i=1}^{\tilde{s}^{[\ell]}} b_i^{[\ell]} \mathcal{F}^{[\ell]}(t_n + c_i^{[\ell,\ell]} \Delta t, \mathbf{Y}_i^{[\ell]}), \quad (7a)$$

$$\mathbf{Y}_i^{[\ell]} = \mathbf{y}_n + \Delta t \sum_{\ell'=1}^{N'} \sum_{j=1}^{\tilde{s}^{[\ell]}} a_{ij}^{[\ell',\ell]} \mathcal{F}^{[\ell']}(t_n + c_j^{[\ell',\ell]} \Delta t, \mathbf{Y}_j^{[\ell']}). \quad (7b)$$

The corresponding generalized Butcher tableau is

$$\begin{array}{cccc|cccc|c} \mathbf{c}^{[1,1]} & \mathbf{c}^{[1,2]} & \dots & \mathbf{c}^{[1,N]} & \mathbf{A}^{[1,1]} & \mathbf{A}^{[1,2]} & \dots & \mathbf{A}^{[1,N]} \\ \mathbf{c}^{[2,1]} & \mathbf{c}^{[2,2]} & \dots & \mathbf{c}^{[2,N]} & \mathbf{A}^{[2,1]} & \mathbf{A}^{[2,2]} & \dots & \mathbf{A}^{[2,N]} \\ \vdots & \vdots & \ddots & \vdots & \vdots & \vdots & \ddots & \vdots \\ \mathbf{c}^{[N',1]} & \mathbf{c}^{[N',2]} & \dots & \mathbf{c}^{[N',N]} & \mathbf{A}^{[N',1]} & \mathbf{A}^{[N',2]} & \dots & \mathbf{A}^{[N',N]} \\ \hline & & & & \mathbf{b}^{[1]} & \mathbf{b}^{[2]} & \dots & \mathbf{b}^{[N]} \end{array} \quad (8)$$

Remark 2. GARK methods generalize the structure of ARK methods in the sense that different operators of the right-hand side of eq. (1) can be integrated by Runge–Kutta methods with different numbers of stages. The diagonal matrix $\mathbf{A}^{[\ell,\ell]}$ corresponds to the Runge–Kutta method used to integrate operator ℓ . The off-diagonal matrices $\mathbf{A}^{[\ell',\ell]}, \ell' \neq \ell$, represent the coupling between operators within a stage.

Definition 2.4 (internal consistency of GARK methods). A GARK method eq. (7) is called internally consistent Sandu and Günther [2015] if

$$\sum_{j=1}^{\tilde{s}^{[\ell]}} a_{ij}^{[\ell',1]} = \dots = \sum_{j=1}^{\tilde{s}^{[N]}} a_{ij}^{[\ell',N]} = c_i^{[\ell',\ell]}, \quad i = 1, 2, \dots, \tilde{s}^{[\ell']}, \ell' = 1, 2, \dots, N'. \quad (9)$$

Remark 3. The internal consistency condition eq. (9) ensures that all intermediate stages are computed at the same internal times. If a method is internally consistent, the matrix $[\mathbf{c}^{[i,j]}], i = 1, 2, \dots, N', j = 1, 2, \dots, N$ in eq. (8) can be represented as a single column $[\mathbf{c}^{[1,1]}, \mathbf{c}^{[2,2]}, \dots, \mathbf{c}^{[N',N]}]^T$.

As described in Sandu and Günther [2015], any GARK method can be written as an ARK method (and vice versa) so that the Butcher tableaux for GARK methods (8) can be seen as having the same structure as Butcher tableaux for ARK methods (6).

2.4 FSRK methods

When solving (1), one can use operator-splitting methods combined with suitable Runge–Kutta methods to integrate each operator. We call this an FSRK method as defined below.

Definition 2.5 (FSRK methods). Consider (1), and assume that we advance the time integration by choosing a combination of an s -stage OS method and Runge–Kutta time-stepping methods. Let $\{\alpha_k^{[\ell]}\}_{k=1,2,\dots,s}^{l=1,2,\dots,N}$ be the coefficients of the OS method. Let $\begin{array}{c|c} \tilde{\mathbf{c}}_k^{[\ell]} & \tilde{\mathbf{A}}_k^{[\ell]} \\ \hline & \tilde{\mathbf{b}}_k^{[\ell]} \end{array}$ be the Butcher tableau of the $\tilde{s}_k^{[\ell]}$ -stage Runge–Kutta method applied to operator l at OS stage k .

Then, one step of an FSRK methods reads

$$\mathbf{y}_{n+1} = \mathbf{y}_n + \Delta t \sum_{k=1}^s \sum_{\ell=1}^N \sum_{i=1}^{\tilde{s}_k^{[\ell]}} b_{k,i}^{[\ell]} \mathcal{F}^{[\ell]}(t_n + c_{k,i}^{[\ell]} \Delta t, \mathbf{Y}_{k,i}^{[\ell]}), \quad (10a)$$

$$\mathbf{Y}_{k,i}^{[\ell]} = \mathbf{y}_n + \Delta t \sum_{k=1}^s \sum_{\ell'=1}^N \sum_{j=1}^{\tilde{s}_k^{[\ell']}} a_{k,ij}^{[\ell,\ell']} \mathcal{F}^{[\ell']}(t_n + c_{k,j}^{[\ell']} \Delta t, \mathbf{Y}_{k,j}^{[\ell']}), \quad (10b)$$

$$\text{where } a_{k,ij}^{[\ell,\ell']} = \begin{cases} 0, & \text{if } \ell < \ell', \\ \alpha_k^{[\ell']} \tilde{a}_{k,ij}^{[\ell']}, & \text{if } \ell = \ell', \\ \alpha_k^{[\ell']} \tilde{b}_{k,j}^{[\ell']}, & \text{if } \ell > \ell', \end{cases} \quad b_{k,i}^{[\ell]} = \alpha_k^{[\ell]} \tilde{b}_{k,i}^{[\ell]}, \text{ and } c_{k,i}^{[\ell]} = \sum_{j=1}^{k-1} \alpha_j^{[\ell]} + \alpha_k^{[\ell]} \tilde{c}_{k,i}^{[\ell]}.$$

3 Main results

In this section, we solve (1) using the operator-splitting method (3) where each subsystem $\frac{d\mathbf{y}^{[\ell]}}{dt} = \mathcal{F}^{[\ell]}(t, \mathbf{y}^{[\ell]})$ is integrated using a Runge–Kutta method (4). Because a Runge–Kutta method is applied to a subsystem that is usually solved over a fraction, $\alpha_k^{[\ell]}$, of Δt , this results in an FSRK method. We show that the FSRK can be regarded as a GARK method, present the Butcher tableau associated with it, and analyze its stability.

We first construct the Butcher tableau of an FSRK method in theorem 3.1.

Theorem 3.1. Consider solving (1) with an FSRK method described in definition 2.5. We can construct an extended Butcher tableau with the same structure as (6) that incorporates the coefficients of the Runge–Kutta integrators scaled by the coefficients of the OS method. The extended Butcher tableau is of the form

$$\begin{array}{c|c|c|c|c|c|c|c} \mathbf{c}^{[1]} & \mathbf{c}^{[2]} & \dots & \mathbf{c}^{[N]} & \mathbf{A}^{[1]} & \mathbf{A}^{[2]} & \dots & \mathbf{A}^{[N]} \\ \hline & & & & \mathbf{b}^{[1]} & \mathbf{b}^{[2]} & \dots & \mathbf{b}^{[N]} \end{array}. \quad (11)$$

Let $\mathbb{S}_k^\ell = \sum_{i=1}^{\ell} \tilde{s}_k^{[i]}$ and $\mathbb{S} = \sum_{k=1}^s \mathbb{S}_k^N = \sum_{k=1}^s \sum_{\ell=1}^N \tilde{s}_k^{[\ell]}$. Each matrix $\mathbf{A}^{[\ell]}$ is a block lower-triangular matrix of size $\mathbb{S} \times \mathbb{S}$. Diagonal block k of $\mathbf{A}^{[\ell]}$ is denoted by $\mathbf{A}_k^{[\ell]}$ and is of size $\mathbb{S}_k^N \times \mathbb{S}_k^N$. Each row vector $\mathbf{b}^{[\ell]}$ is a block vector of size $\mathbb{S} \times 1$. Block k of $\mathbf{b}^{[\ell]}$ is denoted by $\mathbf{b}_k^{[\ell]}$. Let $\mathbb{1}$ denote a column vector of ones. The entries of eq. (11) can be written as:

$$\begin{aligned} \mathbf{A}^{[\ell]} &= \begin{bmatrix} \mathbf{A}_1^{[\ell]} & & & & \\ \mathbb{1} \mathbf{b}_1^{[\ell]} & \mathbf{A}_2^{[\ell]} & & & \\ \vdots & \mathbb{1} \mathbf{b}_2^{[\ell]} & \ddots & & \\ \vdots & \vdots & & \ddots & \\ \mathbb{1} \mathbf{b}_1^{[\ell]} & \mathbb{1} \mathbf{b}_2^{[\ell]} & \dots & \mathbb{1} \mathbf{b}_{s-1}^{[\ell]} & \mathbf{A}_s^{[\ell]} \end{bmatrix}, \\ \mathbf{b}^{[\ell]} &= \begin{bmatrix} \mathbf{b}_1^{[\ell]} & \mathbf{b}_2^{[\ell]} & \dots & \mathbf{b}_s^{[\ell]} \end{bmatrix}, \\ \mathbf{c}^{[\ell]} &= \begin{bmatrix} \mathbf{c}_1^{[\ell]} & \mathbf{c}_2^{[\ell]} & \dots & \mathbf{c}_s^{[\ell]} \end{bmatrix}^T, \end{aligned}$$

where

$$\mathbf{A}_k^{[\ell]} = \begin{bmatrix} \mathbf{0}_{\mathbb{S}_k^{\ell-1} \times \mathbb{S}_k^{\ell-1}} & \mathbf{0}_{\mathbb{S}_k^{\ell-1} \times \tilde{\mathbb{S}}_k^{[\ell]}} & \mathbf{0}_{\mathbb{S}_k^{\ell-1} \times (\mathbb{S}_k^N - \mathbb{S}_k^{\ell})} \\ \mathbf{0}_{\tilde{\mathbb{S}}_k^{[\ell]} \times \mathbb{S}_k^{\ell-1}} & \alpha_k^{[\ell]} \tilde{\mathbf{A}}_k^{[\ell]} & \mathbf{0}_{\tilde{\mathbb{S}}_k^{[\ell]} \times (\mathbb{S}_k^N - \mathbb{S}_k^{\ell})} \\ \mathbf{0}_{(\mathbb{S}_k^N - \mathbb{S}_k^{\ell}) \times \mathbb{S}_k^{\ell-1}} & \alpha_k^{[\ell]} \mathbb{1} \tilde{\mathbf{b}}_k^{[\ell]} & \mathbf{0}_{(\mathbb{S}_k^N - \mathbb{S}_k^{\ell}) \times (\mathbb{S}_k^N - \mathbb{S}_k^{\ell})} \end{bmatrix},$$

$$\mathbf{b}_k^{[\ell]} = \begin{bmatrix} \mathbf{0}_{1 \times \mathbb{S}_k^{\ell-1}} & \alpha_k^{[\ell]} \tilde{\mathbf{b}}_k^{[\ell]} & \mathbf{0}_{1 \times (\mathbb{S}_k^N - \mathbb{S}_k^{\ell})} \end{bmatrix},$$

$$\mathbf{c}_k^{[\ell]} = \begin{bmatrix} (\sum_{i=1}^{k-1} \alpha_i^{[\ell]}) \mathbb{1}_{\mathbb{S}_k^{\ell-1}} \\ (\sum_{i=1}^{k-1} \alpha_i^{[\ell]}) \mathbb{1}_{\tilde{\mathbb{S}}_k^{[\ell]}} + \alpha_k^{[\ell]} \tilde{\mathbf{c}}_k^{[\ell]} \\ (\sum_{i=1}^k \alpha_i^{[\ell]}) \mathbb{1}_{\mathbb{S}_k^N - \mathbb{S}_k^{\ell}} \end{bmatrix}.$$

Proof. When using the FSRK method, we integrate the N operators over s operator-splitting stages. Therefore, each matrix $\mathbf{A}^{[\ell]}$ is an $s \times s$ block matrix with diagonal blocks $\mathbf{A}_k^{[\ell]}$ of size \mathbb{S}_k^N . Based on the definition of the one-step FSRK method, each block $\mathbf{A}_k^{[\ell]}$ is an $N \times N$ block matrix with the zeros everywhere except on and below diagonal block ℓ . Equation (10b) implies that diagonal block ℓ is of the form $\alpha_k^{[\ell]} \tilde{\mathbf{A}}_k^{[\ell]}$, and the entries below diagonal block ℓ is of the form $\alpha_k^{[\ell]} \tilde{\mathbf{b}}_k^{[\ell]}$. Expressing these matrices explicitly, we have

$$\mathbf{A}^{[\ell]} = \begin{bmatrix} \mathbf{A}_1^{[\ell]} & & & \\ \mathbb{1} \mathbf{b}_1^{[\ell]} & \mathbf{A}_2^{[\ell]} & & \\ \mathbb{1} \mathbf{b}_1^{[\ell]} & \mathbb{1} \mathbf{b}_2^{[\ell]} & \ddots & \\ \vdots & \vdots & & \ddots \\ \mathbb{1} \mathbf{b}_1^{[\ell]} & \mathbb{1} \mathbf{b}_2^{[\ell]} & \dots & \dots & \mathbf{A}_s^{[\ell]} \end{bmatrix},$$

where

$$\mathbf{A}_k^{[\ell]} = \begin{bmatrix} \mathbf{0}_{\mathbb{S}_k^{\ell-1} \times \mathbb{S}_k^{\ell-1}} & \mathbf{0}_{\mathbb{S}_k^{\ell-1} \times \tilde{\mathbb{S}}_k^{[\ell]}} & \mathbf{0}_{\mathbb{S}_k^{\ell-1} \times (\mathbb{S}_k^N - \mathbb{S}_k^{\ell})} \\ \mathbf{0}_{\tilde{\mathbb{S}}_k^{[\ell]} \times \mathbb{S}_k^{\ell-1}} & \alpha_k^{[\ell]} \tilde{\mathbf{A}}_k^{[\ell]} & \mathbf{0}_{\tilde{\mathbb{S}}_k^{[\ell]} \times (\mathbb{S}_k^N - \mathbb{S}_k^{\ell})} \\ \mathbf{0}_{(\mathbb{S}_k^N - \mathbb{S}_k^{\ell}) \times \mathbb{S}_k^{\ell-1}} & \alpha_k^{[\ell]} \mathbb{1} \tilde{\mathbf{b}}_k^{[\ell]} & \mathbf{0}_{(\mathbb{S}_k^N - \mathbb{S}_k^{\ell}) \times (\mathbb{S}_k^N - \mathbb{S}_k^{\ell})} \end{bmatrix},$$

$$\mathbf{b}_k^{[\ell]} = \begin{bmatrix} \mathbf{0}_{1 \times \mathbb{S}_k^{\ell-1}} & \alpha_k^{[\ell]} \tilde{\mathbf{b}}_k^{[\ell]} & \mathbf{0}_{1 \times (\mathbb{S}_k^N - \mathbb{S}_k^{\ell})} \end{bmatrix}.$$

Equation (10a) implies that

$$\mathbf{b}^{[\ell]} = \begin{bmatrix} \mathbf{b}_1^{[\ell]} & \mathbf{b}_2^{[\ell]} & \dots & \mathbf{b}_s^{[\ell]} \end{bmatrix},$$

$$\mathbf{c}^{[\ell]} = \begin{bmatrix} \mathbf{c}_1^{[\ell]} & \mathbf{c}_2^{[\ell]} & \dots & \mathbf{c}_s^{[\ell]} \end{bmatrix}^T,$$

where

$$\mathbf{b}_k^{[\ell]} = \begin{bmatrix} \mathbf{0}_{1 \times \mathbb{S}_k^{\ell-1}} & \alpha_k^{[\ell]} \tilde{\mathbf{b}}_k^{[\ell]} & \mathbf{0}_{1 \times (\mathbb{S}_k^N - \mathbb{S}_k^{\ell})} \end{bmatrix},$$

$$\mathbf{c}_k^{[\ell]} = \begin{bmatrix} (\sum_{i=1}^{k-1} \alpha_i^{[\ell]}) \mathbb{1}_{\mathbb{S}_k^{\ell-1}} \\ (\sum_{i=1}^{k-1} \alpha_i^{[\ell]}) \mathbb{1}_{\tilde{\mathbb{S}}_k^{[\ell]}} + \alpha_k^{[\ell]} \tilde{\mathbf{c}}_k^{[\ell]} \\ (\sum_{i=1}^k \alpha_i^{[\ell]}) \mathbb{1}_{\mathbb{S}_k^N - \mathbb{S}_k^{\ell}} \end{bmatrix}.$$

Combining all the coefficients together, block ℓ is written as

$$\begin{array}{c|c}
\begin{array}{c|c|c|c|c|c}
0 & 0 & \cdots & 0 & & \\
\alpha_1^{[\ell]} \tilde{\mathbf{c}}_1^{[\ell]} & \vdots & \alpha_1^{[\ell]} \tilde{\mathbf{A}}_1^{[\ell]} & \vdots & & \\
\alpha_1^{[\ell]} \mathbb{1} & \vdots & \alpha_1^{[\ell]} \mathbb{1} \tilde{\mathbf{b}}_1^{[\ell]} & \vdots & & \\
\vdots & \vdots & \vdots & & & \\
\vdots & \vdots & \alpha_1^{[\ell]} \mathbb{1} \tilde{\mathbf{b}}_1^{[\ell]} & 0 & \cdots & 0 \\
\alpha_1^{[\ell]} \mathbb{1} + \alpha_2^{[\ell]} \tilde{\mathbf{c}}_2^{[\ell]} & \vdots & \vdots & \vdots & \alpha_2^{[\ell]} \tilde{\mathbf{A}}_2^{[\ell]} & \vdots \\
(\alpha_1^{[\ell]} + \alpha_2^{[\ell]}) \mathbb{1} & \vdots & \vdots & \vdots & \alpha_2^{[\ell]} \mathbb{1} \tilde{\mathbf{b}}_2^{[\ell]} & \vdots \\
\vdots & \vdots & \vdots & \vdots & \vdots & \vdots \\
\hline
\mathbf{c}^{[\ell]} & \mathbf{A}^{[\ell]} & \vdots & \vdots & \vdots & \ddots \\
\hline
& \mathbf{b}^{[\ell]} & \vdots & \vdots & \vdots & \ddots \\
\hline
& & \vdots & \vdots & \vdots & \ddots \\
\hline
& (\sum_{i=1}^{s-1} \alpha_i^{[\ell]}) \mathbb{1} & \alpha_1^{[\ell]} \mathbb{1} \tilde{\mathbf{b}}_1^{[\ell]} & \alpha_2^{[\ell]} \mathbb{1} \tilde{\mathbf{b}}_2^{[\ell]} & \vdots & \ddots & 0 & \cdots & 0 \\
& (\sum_{i=1}^{s-1} \alpha_i^{[\ell]}) \mathbb{1} + \alpha_s^{[\ell]} \tilde{\mathbf{c}}_s^{[\ell]} & \vdots & \vdots & \vdots & \ddots & \vdots & \alpha_s^{[\ell]} \tilde{\mathbf{A}}_s^{[\ell]} & \vdots \\
& \sum_{i=1}^s \alpha_i^{[\ell]} & \vdots & \vdots & \vdots & \ddots & \vdots & \alpha_s^{[\ell]} \mathbb{1} \tilde{\mathbf{b}}_s^{[\ell]} & \vdots \\
& \vdots & \vdots & \vdots & \vdots & \ddots & \vdots & \vdots & \vdots \\
& \sum_{i=1}^s \alpha_i^{[\ell]} & 0 & \alpha_1^{[\ell]} \mathbb{1} \tilde{\mathbf{b}}_1^{[\ell]} & 0 & 0 & \alpha_2^{[\ell]} \mathbb{1} \tilde{\mathbf{b}}_2^{[\ell]} & 0 & \cdots & 0 & \alpha_s^{[\ell]} \mathbb{1} \tilde{\mathbf{b}}_s^{[\ell]} & 0 \\
\hline
& & 0 & \alpha_1^{[\ell]} \mathbb{1} \tilde{\mathbf{b}}_1^{[\ell]} & 0 & 0 & \alpha_2^{[\ell]} \mathbb{1} \tilde{\mathbf{b}}_2^{[\ell]} & 0 & \cdots & 0 & \alpha_s^{[\ell]} \mathbb{1} \tilde{\mathbf{b}}_s^{[\ell]} & 0
\end{array} & \quad (12)
\end{array}$$

Remark 4. An example of the extended Butcher tableau is given in eq. (13). Essentially, in each block $A_k^{[\ell]}$, the zeros are padding for operators other than operator ℓ that is being integrated. A more compact form of the Butcher tableau that removes the zero padding and combines the $A^{[\ell]}$ to reveal the block lower-triangular structure is given in eq. (14). The diagonal blocks of the compact tableau have the same structure as eq. (8). Each diagonal block of eq. (14) is a block lower-triangular matrix that shows the specific structured coupling between the operators of an FSRK method. As expected, the coupling between operators is more restrictive than a general GARK method. We note that many published FSRK methods are not internally consistent. Even if after each stage all the operators have the same abscissae, internal consistency may fail at the stages of the Runge–Kutta sub-integrators.

Remark 5. Our construction of the extended Butcher tableau uses the OS method eq. (3). The rows of the tableaux assume the intermediate variables $\mathbf{Y}_{k,i}^{[\ell]}$ are ordered as they appear in the FSRK method, i.e., $\mathbf{Y}_{1,1:\tilde{s}_1^{[1]}}^{[1]}, \dots, \mathbf{Y}_{1,1:\tilde{s}_1^{[N]}}^{[N]}, \dots, \mathbf{Y}_{s,1:\tilde{s}_s^{[1]}}^{[1]}, \dots, \mathbf{Y}_{s,1:\tilde{s}_s^{[N]}}^{[N]}$. If an operator-splitting method is constructed by composing eq. (2a) and eq. (2b) over fractions of Δt , then the intermediate variables $\mathbf{Y}_{k,i}^{[\ell]}$ should be re-ordered in the order they are applied to obtain an extended Butcher tableau in the same structure as presented in theorem 3.1. In González-Pinto et al. [2022], Butcher tableaux for two special FSRKs are shown. The first one was for the second-order Strang splitting method, and the second one was for the fourth-order Yoshida splitting method. Both examples assume the same Runge–Kutta method is applied to every operator at each stage, and the intermediate variables are ordered as $\mathbf{Y}_{1,1:\tilde{s}_1^{[1]}}^{[1]}, \dots, \mathbf{Y}_{s,1:\tilde{s}_s^{[1]}}^{[1]}, \dots, \mathbf{Y}_{1,1:\tilde{s}_1^{[N]}}^{[N]}, \dots, \mathbf{Y}_{s,1:\tilde{s}_s^{[N]}}^{[N]}$. For example, suppose a 3-additive ODE is solved using the Strang splitting method

$$\varphi_{\Delta t/2}^{[1]} \circ \varphi_{\Delta t/2}^{[2]} \circ \varphi_{\Delta t/2}^{[3]} \circ \varphi_{\Delta t/2}^{[3]} \circ \varphi_{\Delta t/2}^{[2]} \circ \varphi_{\Delta t/2}^{[1]},$$

where each operator is solved with the same s -stage Runge–Kutta method with Butcher tableau $\frac{\mathbf{c}}{\mathbf{b}} \mid \mathbf{A}$. The compact version of the extended Butcher tableau constructed using theorem 3.1 is

	$\mathbf{Y}_{1,1:s}^{[1]}$	$\mathbf{Y}_{1,1:s}^{[2]}$	$\mathbf{Y}_{1,1:s}^{[3]}$	$\mathbf{Y}_{2,1:s}^{[3]}$	$\mathbf{Y}_{2,1:s}^{[2]}$	$\mathbf{Y}_{1,1:s}^{[1]}$
$\mathbf{Y}_{1,1:s}^{[1]}$	$\frac{1}{2}\mathbf{A}$					
$\mathbf{Y}_{1,1:s}^{[2]}$	$\frac{1}{2}\mathbf{1b}$	$\frac{1}{2}\mathbf{A}$				
$\mathbf{Y}_{1,1:s}^{[3]}$	$\frac{1}{2}\mathbf{1b}$	$\frac{1}{2}\mathbf{1b}$	$\frac{1}{2}\mathbf{A}$			
$\mathbf{Y}_{2,1:s}^{[3]}$	$\frac{1}{2}\mathbf{1b}$	$\frac{1}{2}\mathbf{1b}$	$\frac{1}{2}\mathbf{1b}$	$\frac{1}{2}\mathbf{A}$		
$\mathbf{Y}_{2,1:s}^{[2]}$	$\frac{1}{2}\mathbf{1b}$	$\frac{1}{2}\mathbf{1b}$	$\frac{1}{2}\mathbf{1b}$	$\frac{1}{2}\mathbf{1b}$	$\frac{1}{2}\mathbf{A}$	
$\mathbf{Y}_{2,1:s}^{[1]}$	$\frac{1}{2}\mathbf{1b}$	$\frac{1}{2}\mathbf{1b}$	$\frac{1}{2}\mathbf{1b}$	$\frac{1}{2}\mathbf{1b}$	$\frac{1}{2}\mathbf{1b}$	$\frac{1}{2}\mathbf{A}$

Each diagonal block of eq. (15) has the structure eq. (8). The Butcher tableau for the same method presented in González-Pinto et al. [2022] is

	$\mathbf{Y}_{1,1:s}^{[1]}$	$\mathbf{Y}_{2,1:s}^{[1]}$	$\mathbf{Y}_{1,1:s}^{[2]}$	$\mathbf{Y}_{2,1:s}^{[2]}$	$\mathbf{Y}_{1,1:s}^{[3]}$	$\mathbf{Y}_{2,1:s}^{[3]}$
$\mathbf{Y}_{1,1:s}^{[1]}$	$\frac{1}{2}\mathbf{A}$					
$\mathbf{Y}_{2,1:s}^{[1]}$	$\frac{1}{2}\mathbf{1b}$	$\frac{1}{2}\mathbf{A}$	$\frac{1}{2}\mathbf{1b}$	$\frac{1}{2}\mathbf{1b}$	$\frac{1}{2}\mathbf{1b}$	$\frac{1}{2}\mathbf{1b}$
$\mathbf{Y}_{1,1:s}^{[2]}$	$\frac{1}{2}\mathbf{1b}$		$\frac{1}{2}\mathbf{A}$			
$\mathbf{Y}_{2,1:s}^{[2]}$	$\frac{1}{2}\mathbf{1b}$		$\frac{1}{2}\mathbf{1b}$	$\frac{1}{2}\mathbf{A}$	$\frac{1}{2}\mathbf{1b}$	$\frac{1}{2}\mathbf{1b}$
$\mathbf{Y}_{1,1:s}^{[3]}$	$\frac{1}{2}\mathbf{1b}$		$\frac{1}{2}\mathbf{1b}$		$\frac{1}{2}\mathbf{A}$	
$\mathbf{Y}_{2,1:s}^{[3]}$	$\frac{1}{2}\mathbf{1b}$		$\frac{1}{2}\mathbf{1b}$		$\frac{1}{2}\mathbf{1b}$	$\frac{1}{2}\mathbf{A}$

We note that the entire tableau eq. (16) has the structure eq. (8). We further note that the tableaux presented in González-Pinto et al. [2022] have the same structure as the compact Butcher tableau eq. (14) after re-ordering the intermediate variables $\mathbf{Y}_{k,i}^{[\ell]}$. Note that our format has a few advantages in implementation: it is easier to arrange data row-by-row in the order they appear and solve for $\mathbf{Y}_{k,i}^{[\ell]}$ when using a block lower-triangular matrix.

Because the FSRK method has the structure of a GARK method, we can study its stability in the GARK framework. Theorem 3.2 presents the main result on the stability function of an FSRK method.

Theorem 3.2. We apply the FSRK method (10) to the linear test equation

$$\frac{dy}{dt} = \sum_{\ell=1}^N \lambda^{[\ell]} y. \quad (17)$$

We define $z^{[\ell]} = \Delta t \lambda^{[\ell]}$ and the stability function of each Runge–Kutta method used to integrate each operator to be $R_k^{[\ell]}(z^{[\ell]})$, $\ell = 1, 2, \dots, N$, $k = 1, 2, \dots, s$. Then the stability function $R(z^{[1]}, z^{[2]}, \dots, z^{[N]})$ of the FSRK method is given by

$$R(z^{[1]}, z^{[2]}, \dots, z^{[N]}) = \prod_{k=1}^s \prod_{\ell=1}^N R_k^{[\ell]}(\alpha_k^{[\ell]} z^{[\ell]}).$$

That is, *the stability function of the FSRK method applied to eq. (17) is the product of the stability functions of the individual RK methods with arguments scaled by the OS method coefficients.*

Proof. Assume that we apply a Runge–Kutta method to the operator $\mathcal{F}^{[\ell]}$ at stage k of the FS method. We refer to this Runge–Kutta method as $\text{RK}_k^{[\ell]}$ with corresponding Butcher tableau

$$\begin{array}{c|c} \tilde{\mathbf{c}}_k^{[\ell]} & \tilde{\mathbf{A}}_k^{[\ell]} \\ \hline & \tilde{\mathbf{b}}_k^{[\ell]} \end{array}.$$

Let $R_k^{[\ell]}(z^{[\ell]})$ be the stability function corresponds to $\text{RK}_k^{[\ell]}$.

Let $y_k^{[\ell]}$ be the intermediate solution after solving $\frac{dy^{[\ell]}}{dt} = \lambda^{[\ell]} y^{[\ell]}$ at stage k .

Therefore, after solving $\frac{dy^{[1]}}{dt} = \lambda^{[1]} y^{[1]}$ at stage 1,

$$y_1^{[1]} = R_1^{[1]}(\alpha_1^{[1]} z^{[1]}) y_n,$$

and after solving $\frac{dy^{[N]}}{dt} = \lambda^{[N]} y^{[N]}$ at stage 1,

$$y_1^{[N]} = \left(\prod_{\ell=1}^N R_1^{[\ell]}(\alpha_1^{[\ell]} z^{[\ell]}) \right) y_n.$$

By repeating this process over all operators and stages, we can write y_{n+1} as

$$y_{n+1} = y_s^{[N]} = \left(\prod_{k=1}^s \prod_{\ell=1}^N R_k^{[\ell]}(\alpha_k^{[\ell]} z^{[\ell]}) \right) y_n.$$

□

Remark 6. Theorem 3.2 is a generalization of simpler, lower-order results found in Hundsdorfer and Verwer [2003], Ropp and Shadid [2005, 2009].

Remark 7. The FSRK method (10) can be described using the extended Butcher tableau (13) which has the structure of an ARK method. Using example 4 in Sandu and Günther [2015], the stability function can be written as

$$R(z^{[1]}, z^{[2]}, \dots, z^{[N]}) = 1 + \left(\sum_{\ell=1}^N z^{[\ell]} \mathbf{b}^{[\ell]} \right) \cdot \left(\mathbf{I}_{\mathbb{S} \times \mathbb{S}} - \left(\sum_{\ell=1}^N z^{[\ell]} \mathbf{A}^{[\ell]} \right) \right)^{-1} \cdot \mathbb{1}_{\mathbb{S}},$$

where $\mathbf{A}^{[\ell]}$ and $\mathbf{b}^{[\ell]}$ are as defined in the extended Butcher tableau in theorem 3.1, $\mathbb{1}$ is the vector of ones, and $\mathbb{S} = \sum_{k=1}^s \mathbb{S}_k^N = \sum_{k=1}^s \sum_{\ell=1}^N \tilde{s}_k^{[\ell]}$.

Remark 8. If we change the order of the sub-integrators, the stability function of the FSRK method is generally changed, even without changing the Runge–Kutta methods used for each operator, because the coefficients $\alpha_k^{[\ell]}$ associated with each sub-integrator are generally changed. This can explain observations of different stability behaviour of numerical methods depending on order of sub-integration, e.g., Torabi Ziaratgahi et al. [2014], Ropp et al. [2004]. See also examples below.

Remark 9. The choice of test equation eq. (17) assumes that the Jacobians of each operator with respect to the solution \mathbf{y} are simultaneously diagonalizable in a neighbourhood of the solution. It is well known that this assumption may not lead to useful practical analysis. Accordingly, more elaborate test equations exist Gear [1974], Kværnø [2000]; however, there is no generally accepted test equation that is considered standard at this time. Nonetheless, eq. (17) is often useful in practice and in fact may be appropriate as a test equation for co-simulation.

4 Numerical Examples

In this section, we illustrate some of the results presented in this paper, their implications, and how they can be used to explain various observations and loose ends in the literature. We show how to construct the Butcher tableau for a general FSRK method with different RK methods for each operator and each OS stage, how stability depends on the splitting (the choice of operators, their order of integration, and sub-integrators). Of particular interest is how backward sub-steps manifest themselves as holes in the stability region; we describe the extent to which backward steps may destabilize a computation and how such destabilization can be mitigated.

4.1 Construction of the extended Butcher tableau

Example 1. We first present a simple example to construct a general extended Butcher tableau. Consider the problem

$$\frac{dy}{dt} = \mathcal{F}^{[1]}(t, y) + \mathcal{F}^{[2]}(t, y) + \mathcal{F}^{[3]}(t, y).$$

We solve the problem using a three-stage, second-order, 3-operator-splitting method $OS_3(3,2)$ whose coefficients are given in table 1. The first sub-equation $\frac{dy^{[1]}}{dt} = \mathcal{F}^{[1]}(t, y^{[1]})$ is integrated using the forward Euler (FE), backward

Table 1: Coefficients $\alpha_k^{[i]}$ for a three-stage, second-order, 3-OS method $OS_3(3,2)$

k	$\alpha_k^{[1]}$	$\alpha_k^{[2]}$	$\alpha_k^{[3]}$
1	1/3	1	1/4
2	1/3	-1/2	1
3	1/3	1/2	-1/4

Euler (BE), and Heun methods at stages $k = 1, 2, 3$ respectively. The second sub-equation $\frac{dy^{[2]}}{dt} = \mathcal{F}^{[2]}(t, y^{[2]})$ is integrated using the Crank–Nicolson, BE, and FE methods at stages $k = 1, 2, 3$ respectively. The third sub-equation $\frac{dy^{[3]}}{dt} = \mathcal{F}^{[3]}(t, y^{[3]})$ is integrated using the BE, BE, and FE methods at stages $k = 1, 2, 3$ respectively. The Butcher tableaux of these methods at each stage is given in eq. (18).

$$\begin{array}{c|cc} \tilde{\mathbf{c}}_1^{[1]} & \tilde{\mathbf{A}}_1^{[1]} \\ \hline \tilde{\mathbf{b}}_1^{[1]} & 0 & 1 \end{array} = \begin{array}{c|c} 0 & 0 \\ \hline 1 & \end{array}, \quad \begin{array}{c|cc} \tilde{\mathbf{c}}_1^{[2]} & \tilde{\mathbf{A}}_1^{[2]} \\ \hline \tilde{\mathbf{b}}_1^{[2]} & 0 & 0 \\ & 1/2 & 1/2 \\ & 1/2 & 1/2 \end{array} = \begin{array}{c|cc} 0 & 0 & 0 \\ \hline 1 & 1/2 & 1/2 \\ 1/2 & 1/2 & 1/2 \end{array}, \quad \begin{array}{c|cc} \tilde{\mathbf{c}}_1^{[3]} & \tilde{\mathbf{A}}_1^{[3]} \\ \hline \tilde{\mathbf{b}}_1^{[3]} & 1 & 1 \end{array} = \begin{array}{c|c} 1 & 1 \\ \hline 1 & 1 \end{array} \\ \begin{array}{c|cc} \tilde{\mathbf{c}}_2^{[1]} & \tilde{\mathbf{A}}_2^{[1]} \\ \hline \tilde{\mathbf{b}}_2^{[1]} & 1 & 1 \\ & 1 & \end{array} = \begin{array}{c|cc} 1 & 1 & 0 \\ \hline 1 & 1 & 0 \\ 0 & 0 & 1 \end{array}, \quad \begin{array}{c|cc} \tilde{\mathbf{c}}_2^{[2]} & \tilde{\mathbf{A}}_2^{[2]} \\ \hline \tilde{\mathbf{b}}_2^{[2]} & 1 & 1 \\ & 1 & \end{array} = \begin{array}{c|cc} 1 & 1 & 0 \\ \hline 1 & 1 & 0 \\ 0 & 0 & 1 \end{array}, \quad \begin{array}{c|cc} \tilde{\mathbf{c}}_2^{[3]} & \tilde{\mathbf{A}}_2^{[3]} \\ \hline \tilde{\mathbf{b}}_2^{[3]} & 1 & 1 \\ & 1 & \end{array} = \begin{array}{c|cc} 1 & 1 & 0 \\ \hline 1 & 1 & 0 \\ 0 & 0 & 1 \end{array}, \quad (18) \\ \begin{array}{c|ccc} \tilde{\mathbf{c}}_3^{[1]} & \tilde{\mathbf{A}}_3^{[1]} & 0 & 0 \\ \hline \tilde{\mathbf{b}}_3^{[1]} & 1 & 1 & 0 \\ & 1/2 & 1/2 & \end{array} = \begin{array}{c|ccc} 0 & 0 & 0 & 0 \\ \hline 1 & 1 & 0 & 0 \\ 1/2 & 1/2 & 1 & 0 \end{array}, \quad \begin{array}{c|cc} \tilde{\mathbf{c}}_3^{[2]} & \tilde{\mathbf{A}}_3^{[2]} \\ \hline \tilde{\mathbf{b}}_3^{[2]} & 0 & 0 \\ & 1 & \end{array} = \begin{array}{c|cc} 0 & 0 & 0 \\ \hline 0 & 1 & 0 \end{array}, \quad \begin{array}{c|cc} \tilde{\mathbf{c}}_3^{[3]} & \tilde{\mathbf{A}}_3^{[3]} \\ \hline \tilde{\mathbf{b}}_3^{[3]} & 0 & 0 \\ & 0 & 1 \end{array} = \begin{array}{c|cc} 0 & 0 & 0 \\ \hline 0 & 0 & 1 \end{array}. \end{array}$$

The extended Butcher tableau consists of three major sections $\mathbf{A}^{[1]}$, $\mathbf{A}^{[2]}$, and $\mathbf{A}^{[3]}$. Each matrix $\mathbf{A}^{[\ell]}$ is of size $\mathbb{S} \times \mathbb{S}$, where $\mathbb{S} = \sum_{k=1}^3 \sum_{\ell=1}^3 \tilde{s}_k^{[\ell]} = 11$. In the following tableaux, the blue numbers correspond to $\alpha_k^{[\ell]} \tilde{\mathbf{A}}_k^{[\ell]}$.

$$\frac{\mathbf{c}^{[2]} \mid \mathbf{A}^{[2]}}{\mathbf{b}^{[2]}} = \begin{array}{c|ccccc|c|ccccc} \mathbf{Y}_{1,1}^{[1]} & 0 & 0 & 0 & 0 & \vdots & & & & & & & \\ \mathbf{Y}_{1,1}^{[2]} & 0 & \vdots & \mathbf{0} & \mathbf{0} & \vdots & & & & & & & \\ \mathbf{Y}_{1,2}^{[2]} & 1 & \vdots & \mathbf{1/2} & \mathbf{1/2} & \vdots & & & & & & & \\ \hline \mathbf{Y}_{1,1}^{[3]} & 1 & \vdots & 1/2 & 1/2 & \vdots & & & & & & & \\ \hline \mathbf{Y}_{2,1}^{[1]} & 1 & \vdots & 1/2 & 1/2 & \vdots & 0 & 0 & 0 & & & & \\ \mathbf{Y}_{2,1}^{[2]} & 1/2 & \vdots & 1/2 & 1/2 & \vdots & \vdots & \mathbf{-1/2} & \vdots & & & & \\ \mathbf{Y}_{2,1}^{[3]} & 1/2 & \vdots & 1/2 & 1/2 & \vdots & \vdots & \mathbf{-1/2} & \vdots & & & & \\ \hline \mathbf{Y}_{3,1}^{[1]} & 1/2 & \vdots & 1/2 & 1/2 & \vdots & \vdots & \mathbf{-1/2} & \vdots & 0 & 0 & 0 & 0 \\ \mathbf{Y}_{3,2}^{[1]} & 1/2 & \vdots & 1/2 & 1/2 & \vdots & \vdots & \mathbf{-1/2} & \vdots & & & & \\ \hline \mathbf{Y}_{3,1}^{[2]} & 1/2 & \vdots & 1/2 & 1/2 & \vdots & \vdots & \mathbf{-1/2} & \vdots & \vdots & \vdots & \mathbf{0} & \vdots \\ \mathbf{Y}_{3,1}^{[3]} & 1 & 0 & 1/2 & 1/2 & 0 & 0 & -1/2 & 0 & 0 & 0 & 1/2 & 0 \\ \hline & 0 & 1/2 & 1/2 & 0 & 0 & -1/2 & 0 & 0 & 0 & 1/2 & 0 & \end{array}$$

$\mathbf{Y}_{1,1}^{[1]}$	0	0	0	0	0				
$\mathbf{Y}_{1,1}^{[2]}$	0	:	:	:	:				
$\mathbf{Y}_{1,2}^{[2]}$	0	:	:	:	0				
$\mathbf{Y}_{1,1}^{[3]}$	1/4	:	:	:	1/4				
$\mathbf{Y}_{2,1}^{[1]}$	1/4	:	:	:	1/4	0	0	0	
$\mathbf{Y}_{2,1}^{[2]}$	1/4	:	:	:	1/4	:	:	0	
$\mathbf{Y}_{2,1}^{[3]}$	5/4	:	:	:	1/4	:	:	1	
$\mathbf{Y}_{3,1}^{[1]}$	5/4	:	:	:	1/4	:	:	1	0
$\mathbf{Y}_{3,2}^{[1]}$	5/4	:	:	:	1/4	:	:	1	:
$\mathbf{Y}_{3,1}^{[2]}$	5/4	:	:	:	1/4	:	:	1	:
$\mathbf{Y}_{3,1}^{[3]}$	5/4	0	0	0	1/4	0	0	1	0
		0	0	0	1/4	0	0	1	0
						0	0	0	-1/4

The compact tableau is given below. The blue numbers correspond to $\alpha_k^{[\ell]} \tilde{\mathbf{A}}_k^{[\ell]}$.

4.2 Construction of the stability function and linear stability analysis

The next example demonstrates how to construct the stability function from theorem 3.2 and how linear stability analysis can be used to understand some observed stability behaviour when an ODE is solved via an FSRK method. This example also illustrates the how the stability behaviour can depend on the splitting.

Example 2. Consider the differential equation

$$\frac{dy}{dt} = -20y = \lambda^{[1]}y + \lambda^{[2]}y, \quad y(0) = 1. \quad (19)$$

We apply the second-order Strang–Marchuk splitting method to solve eq. (19), where the first sub-equation $\frac{dy}{dt} = \lambda^{[1]}y$ is solved using Heun’s method, and the second sub-equation $\frac{dy}{dt} = \lambda^{[2]}y$ is solved using the two-stage, second-order, L-stable singly diagonally implicit Runge–Kutta method (SDIRK(2,2)).

The stability function for Heun's method is

$$R_{\text{Heun}}(z) = 1 + z + \frac{z^2}{2}.$$

The stability function for the SDIRK(2,2) method is

$$R_{\text{SDIRK}(2,2)}(z) = \frac{z - 2\gamma z + 1}{(\gamma z - 1)^2}, \quad \gamma = \frac{2 - \sqrt{2}}{2}.$$

The stability function for the described FSRK method is

$$R(z^{[1]}, z^{[2]}) = \left[R_{\text{Heun}}\left(\frac{1}{2}z^{[1]}\right) \right]^2 R_{\text{SDIRK}(2,2)}(z^{[2]}).$$

We now consider three different splittings:

- Case 1 (50-50 split): $\lambda^{[1]} = -10$ and $\lambda^{[2]} = -10$. In this case, $z^{[1]} = z^{[2]} = -10\Delta t$. Let $z = -\Delta t$, $z^{[1]} = z^{[2]} = 10z$. The stability region is given by

$$R_{50-50}(z) = \frac{(25z^2/2 + 5z + 1)^2(10z - 20\gamma z + 1)}{(10\gamma z - 1)^2}$$

- Case 2 (10-90 split): $\lambda^{[1]} = -2$ and $\lambda^{[2]} = -18$. Let $z = -\Delta t$, $z^{[1]} = 2z$, $z^{[2]} = 18z$. The stability region is given by

$$R_{10-90}(z) = \frac{(z^2/2 + z + 1)^2(18z - 36\gamma z + 1)}{(18\gamma z - 1)^2}$$

- Case 3 (90-10 split): $\lambda^{[1]} = -18$ and $\lambda^{[2]} = -2$. Let $z = -\Delta t$, $z^{[1]} = 18z$, $z^{[2]} = 2z$. The stability region is given by

$$R_{90-10}(z) = \frac{(81/2 z^2 + 9z + 1)^2(2z - 4\gamma z + 1)}{(2\gamma z - 1)^2}$$

The stability regions $|R_{50-50}(z)| < 1$, $|R_{10-90}(z)| < 1$, and $|R_{90-10}(z)| < 1$ are the interior regions of the curves in fig. 1. The figure confirms the common expectation that the stability of a splitting method is improved when it is possible to treat the stiff part of an ODE with an L-stable method.

4.3 The Brusselator problem

Example 3. In Ropp and Shadid [2005], the instability of the Brusselator problem is explored when solved using the second-order Strang operator-splitting method with the trapezoidal rule for the diffusion term and CVODE Cohen and Hindmarsh [1996] for the reaction term. To analyze the stability in the language of FSRK, we recreate the instability observed in Ropp and Shadid [2005] using the Strang operator-splitting method with Heun’s method as sub-integrators and explain it using the stability function established in theorem 3.2.

The Brusselator problem is defined as follows

$$\frac{\partial T}{\partial t} = D_1 \frac{\partial^2 T}{\partial x^2} + \alpha - (\beta + 1)T + T^2C, \quad (20a)$$

$$\frac{\partial C}{\partial t} = D_2 \frac{\partial^2 C}{\partial x^2} + \beta T - T^2C, \quad (20b)$$

where T and C represent concentrations of different chemical species. In Ropp and Shadid [2005], the authors considered parameter values of $\alpha = 0.6$, $\beta = 2$, and $D_1 = D_2 = \frac{1}{40}$, with boundary conditions $T(0, t) = T(1, t) = \alpha$ and $C(0, t) = C(1, t) = \frac{\beta}{\alpha}$ and initial conditions $T(x, 0) = \alpha + x(1 - x)$ and $C(x, 0) = \frac{\beta}{\alpha} + x^2(1 - x)$. Equation (20) is split according to diffusion and reaction as

$$\begin{aligned} \frac{\partial T}{\partial t} &= D_1 \frac{\partial^2 T}{\partial x^2}, \\ \frac{\partial C}{\partial t} &= D_2 \frac{\partial^2 C}{\partial x^2} \end{aligned}$$

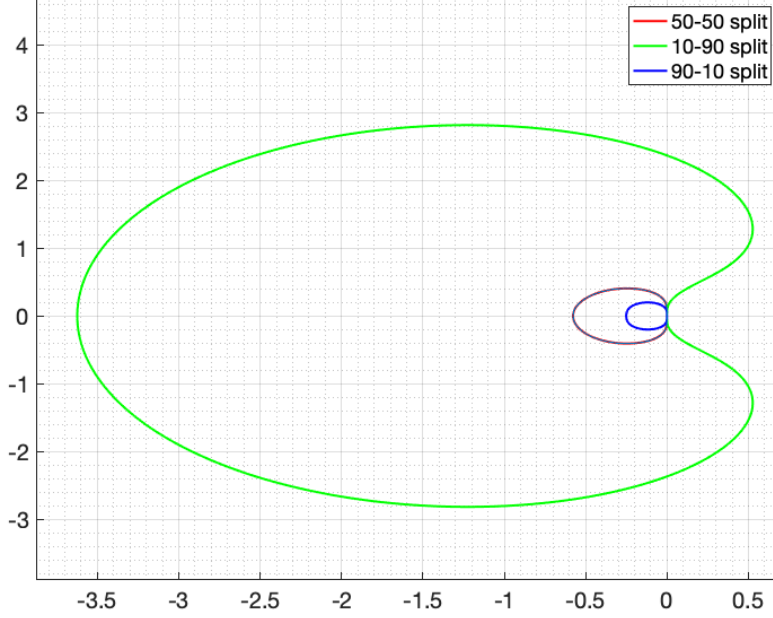


Figure 1: The interior region of each curve is the stability region for the Strang–Marchuk splitting method applied with the Heun and SDIRK(2,2) methods.

and

$$\begin{aligned}\frac{\partial T}{\partial t} &= \alpha - (\beta + 1)T + T^2C, \\ \frac{\partial C}{\partial t} &= \beta T - T^2C.\end{aligned}$$

A reference solution for $t \in [0, 80]$ is computed using the MATLAB parabolic and elliptic PDE solver `pdepe`. We decreased the spatial meshsize Δx and adjusted the absolute and relative tolerances for the solver until there were at least 6 matching digits between successive approximations at 32,000 and 800 uniformly distributed points in space and time, respectively.

For our experiments, the spatial derivatives are discretized using central finite differences on a uniform grid on the interval $x \in [0, 1]$. The ensuing method-of-lines ODEs are then solved using the Strang operator-splitting method with Heun’s method applied to both the reaction and diffusion systems. The unstable behavior is depicted in fig. 2.

To understand this unstable behavior, we consider the stability function of the Strang (Heun+Heun) method using theorem 3.2:

$$\begin{aligned}R(z^{[1]}, z^{[2]}) &= \left[R_{\text{Heun}}\left(\frac{1}{2}z^{[1]}\right) \right]^2 R_{\text{Heun}}(z^{[2]}) \\ &= \left(1 + \frac{1}{2}z^{[1]} + \frac{1}{8}(z^{[1]})^2 \right)^2 \left(1 + z^{[2]} + \frac{1}{2}(z^{[2]})^2 \right),\end{aligned}\tag{21}$$

where $z^{[1]} = \lambda^{[1]}\Delta t$ and $z^{[2]} = \lambda^{[2]}\Delta t$. We compute the eigenvalues of the Jacobian matrices of the diffusion and reaction system. The Jacobian matrix of the diffusion system is

$$J_{\text{Diffusion}} = \begin{bmatrix} D_1 M & 0 \\ 0 & D_2 M \end{bmatrix},$$

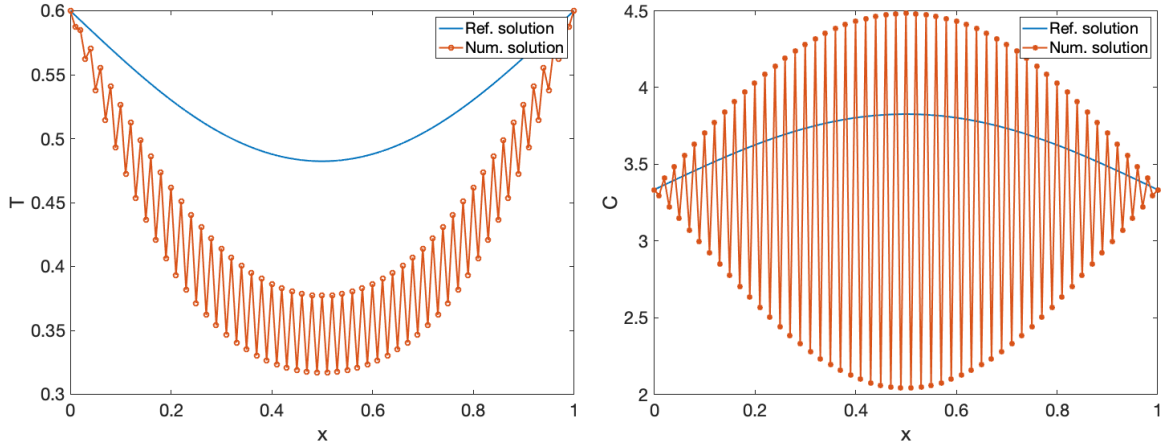


Figure 2: Solution at $t = 80$ using the Strang (Heun+Heun) method with $\Delta t = 0.004001$ and $\Delta x = 0.01$.

where $M = \frac{1}{\Delta x^2} \begin{bmatrix} 0 & \dots & \dots & \dots & 0 \\ 1 & -2 & 1 & & \\ \ddots & \ddots & \ddots & & \\ & 1 & -2 & 1 & \\ 0 & \dots & \dots & \dots & 0 \end{bmatrix}$. The Jacobian matrix of the reaction system is

$$J_{\text{Reaction}} = \begin{bmatrix} 0 & \dots & 0 & 0 & \dots & 0 \\ 0 & -(\beta + 1) + 2T_i C_i & \dots & T_i^2 & & \\ 0 & \dots & \dots & 0 & 0 & \dots \\ 0 & \beta - 2T_i C_i & \dots & -T_i^2 & & \\ 0 & \dots & 0 & 0 & \dots & 0 \end{bmatrix}$$

A plot of the eigenvalues for $t \in [0, 80]$ and $\Delta x = 0.01$ is shown in fig. 3.

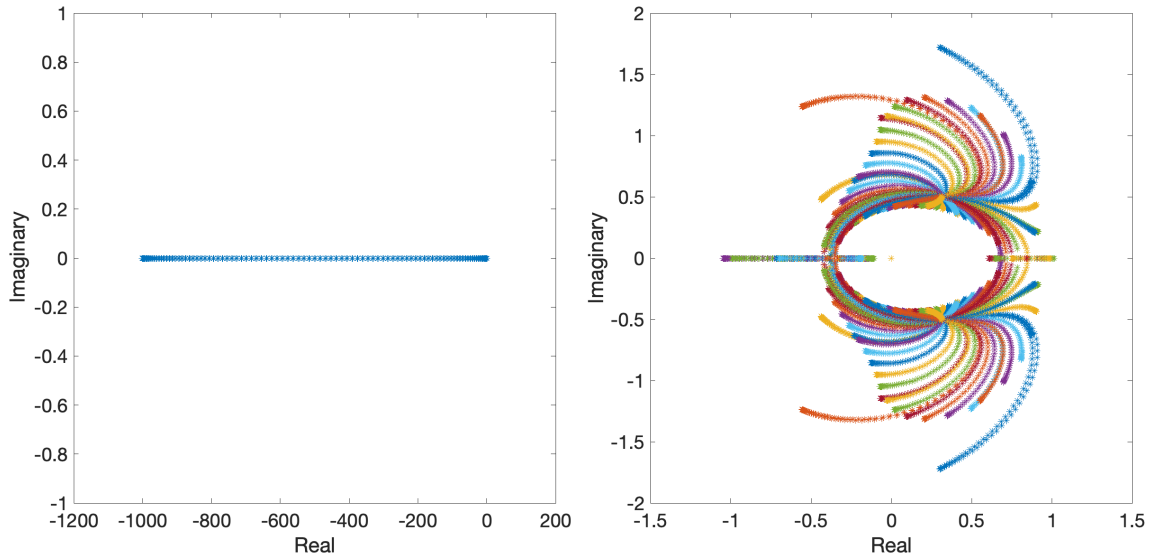


Figure 3: Eigenvalue of the Jacobian matrices $J_{\text{Diffusion}}$ and J_{Reaction} .

Based on the distribution of the eigenvalues and the general shape of the stability region of the Strang (Heun+Heun) OS method, we choose $\lambda^{[1]} = -1000.75$, which is the most negative eigenvalue of the diffusion system, and $\lambda^{[2]} = -1.047$, which is the eigenvalue with the most negative real component of the reaction system. Because the ratio of these two extreme eigenvalues is approximately 1000, we let $z^{[2]} = 0.001z^{[1]}$. The stability function eq. (21) can be written as

$$R(z) = \left(1 + \frac{1}{2}z + \frac{1}{8}z^2\right)^2 \left(1 + 0.001z + \frac{1}{2}(0.001z)^2\right).$$

Based on this stability region, we estimate the largest Δt that produces a stable solution with the Strang (Heun+Heun) method is $\Delta t = 0.004$, agreeing with numerical experiment.

Linear stability regions cannot generally be expected to accurately predict the step-size restriction for stability. However, they can be used to qualitatively compare different FSRK methods. For example, Ropp and Shadid [2005] stated that integrating the diffusion operator with an L-stable method can better control high wave-number instability. The next example explains this observation using stability regions.

We consider a family of SDIRK methods with the following Butcher tableau:

$$\begin{array}{c|cc} \gamma & \gamma & 0 \\ \hline 1-\gamma & 1-2\gamma & \gamma \\ \hline & 1/2 & 1/2 \end{array}, \quad (22)$$

where γ is a free parameter. When $\gamma = 1/2$, the resulting SDIRK method is an A-stable, second-order accurate method. When $\gamma = 1 + 1/\sqrt{2}$, the resulting SDIRK method is an L-stable, second-order method. We solve the Brusselator problem eq. (20) again using the Strang splitting method. The reaction operator is solved with Heun's method, and the diffusion operator is solved in two different ways: once with the A-stable SDIRK method ($\gamma = 1/2$) and then with the L-stable SDIRK method ($\gamma = 1 + 1/\sqrt{2}$). Figure 4 confirms that using an L-stable method with the step-size $\Delta t = 0.02$ improves the stability of the solution. For the parameter values used, the stability region for the FSRK method that uses the A-stable SDIRK method has a negative real intercept of $z \approx -2008$, whereas the one that uses the L-stable SDIRK method is in fact A-stable.

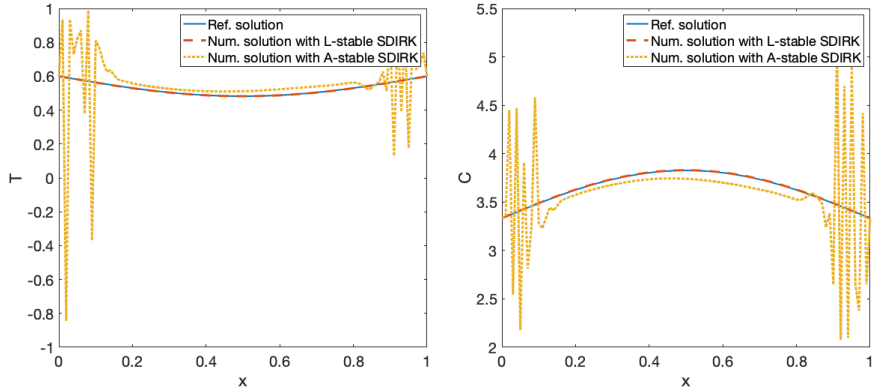


Figure 4: Solutions at $t = 80$ using an A-stable SDIRK method ($\gamma = 1/2$) and an L-stable SDIRK method ($\gamma = 1 + 1/\sqrt{2}$) with $\Delta t = 0.2$.

4.4 Stability regions of FSRK with negative coefficients

OS methods of order three or higher require backward-in-time sub-steps in each operator during the integration Goldman and Kaper [1996]. There is the potential for backward steps to create a hole in the stability region and undermine the stability of the method in practice. We give an example of this phenomenon in example 4.

Example 4. Consider the differential equation

$$\frac{dy}{dt} = \lambda^{[1]}y + \lambda^{[2]}y, \quad y(0) = y_0. \quad (23)$$

Suppose we solve the ODE eq. (23) using the third-order accurate Ruth operator-splitting method whose coefficients are given in table 2. The first operator $\frac{dy}{dt}^{[1]} = \lambda^{[1]}y^{[1]}$ is solved with the three-stage, third-order explicit Runge–Kutta

Table 2: Coefficients $\alpha_k^{[i]}$ for the Ruth method

k	$\alpha_k^{[1]}$	$\alpha_k^{[2]}$
1	$7/24$	$2/3$
2	$3/4$	$-2/3$
3	$-1/24$	1

method due to Kutta (RK3), and the second operator $\frac{dy^{[2]}}{dt} = \lambda^{[2]} y^{[2]}$ is solved with SDIRK(2,3) from eq. (22) with $\gamma = (3 + \sqrt{3})/6$. In the case where $\lambda^{[1]} = \lambda^{[2]}$, the stability function for $z = \lambda^{[1]} \Delta t = \lambda^{[2]} \Delta t$ is

$$R(z) = R_{\text{RK3}}\left(\frac{7}{24}z\right) R_{\text{RK3}}\left(\frac{3}{4}z\right) R_{\text{RK3}}\left(-\frac{1}{24}z\right) \cdot R_{\text{SDIRK}(2,3)}\left(\frac{2}{3}z\right) R_{\text{SDIRK}(2,3)}\left(-\frac{2}{3}z\right) R_{\text{SDIRK}(2,3)}(1z). \quad (24)$$

The stability function for the SDIRK(2,3) method is

$$R_{\text{SDIRK}(2,3)}(z) = 1 - \frac{z^2(2\gamma - 1)}{2(\gamma z - 1)^2} - \frac{z}{\gamma z - 1},$$

from which we see there is a singularity in eq. (24) at $z = 1/(\alpha_k^{[2]} \gamma)$. Such singularities are located in the right-half of the complex plane when $\alpha_k^{[2]} > 0$. When $\alpha_k^{[2]} < 0$, however, the singularity is located in the left-half of the complex plane. In particular, for $\alpha_k^{[\ell]} = -2/3$, the singularity is at $z \approx -1.9$ and results in a hole in the main stability region as shown in fig. 5. In practice, an unfortunate combination of *any* eigenvalue λ and Δt such that $z = \lambda \Delta t \approx -1.9$ would lead to an unstable step and may explain why negative steps have been generally eschewed in practice for non-reversible problems Sornborger and Stewart [1999]. To mitigate this behavior, one could use the implicit method on operators with small negative coefficients $\alpha_k^{[\ell]}$. When $\alpha_k^{[\ell]}$ is sufficiently small, the singularity would be located outside of the stability region. For example, when SDIRK(2,3) is applied to the first operator and the RK3 is applied to the second operator, the singularity in the left-half of the complex plane is located near $z = -30.43$, which is outside the stability region defined by eq. (24) with subscripts RK3 and SDIRK(2,3) interchanged.

5 Conclusions and future work

We have shown how FSRK methods can be systematically represented using Butcher tableaux within the framework of GARK methods. This representation allows us to immediately study their stability properties using an established framework and has further allowed us to provide an informative interpretation of the stability function of an FSRK method in terms of the splitting coefficients, the choice of ordering of the operators, and the underlying RK sub-integrators. These tools enable a systematic explanation and understanding of common observations of FSRK methods in the literature that have only been given as special cases. In particular, we are able to more clearly understand the role of negative splitting coefficients in the overall stability of an FSRK method. The analysis presented in this paper also provide a unified means to develop new OS methods favourable properties. These methods are described elsewhere.

References

- Cláudio Gomes, Casper Thule, David Broman, Peter Gorm Larsen, and Hans Vanherluwe. Co-simulation: A survey. *ACM Comput. Surv.*, 51(3), may 2018. ISSN 0360-0300. doi:10.1145/3179993. URL <https://doi.org/10.1145/3179993>.
- S. Lie and F. Engel. *Theorie der transformationsgruppen (Vol I)*. American Society, Providence, 1970.
- W. Hundsdorfer and J. G. Verwer. *Numerical solution of time-dependent advection-diffusion-reaction equations*, volume 33. Springer-Verlag, Berlin, 2003.
- R. I. McLachlan and G. R. W. Quispel. Splitting methods. *Acta Numerica*, 11:341–434, 2002.
- R. Glowinski, S. J. Osher, and W. Yin. *Splitting Methods in Communication, Imaging, Science, and Engineering*. Springer, 2017.

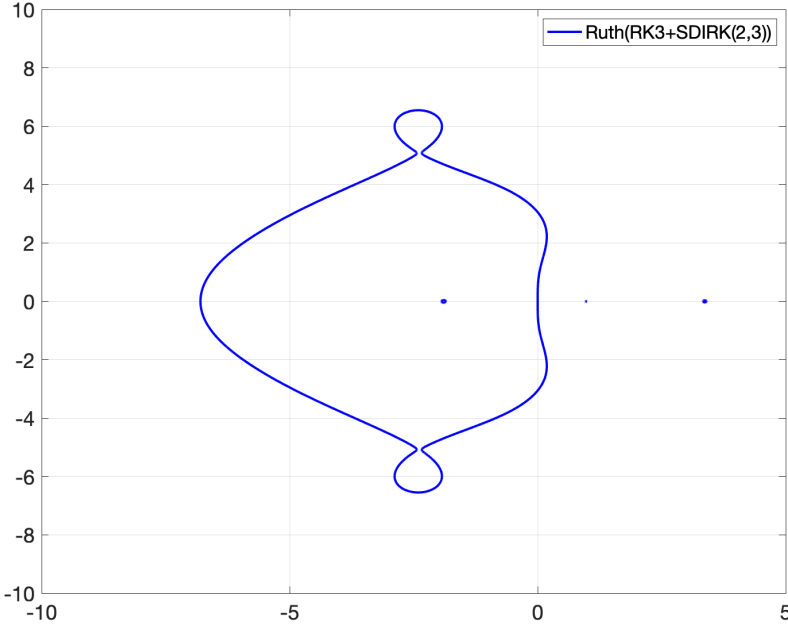


Figure 5: The stability region for the Ruth (RK3+SDIRK2O3) method is the interior of the large contour excluding the hole near $z = -1.9$.

- J. L. Guermond, P. Minev, and J. Shen. An overview of projection methods for incompressible flows. *Comput. Methods Appl. Mech. Engrg.*, 195(44-47):6011–6045, 2006. ISSN 0045-7825. URL <https://doi.org/10.1016/j.cma.2005.10.010>.
- N. N. Yanenko. *The method of fractional steps. The solution of problems of mathematical physics in several variables*. Springer-Verlag, New York-Heidelberg, 1971. Translated from the Russian by T. Cheron. English translation edited by M. Holt.
- H. F. Trotter. Approximation of semi-groups of operators. *Pacific Journal of Mathematics*, 8(4):887–919, 1958.
- S. K. Godunov. A difference method for numerical calculation of discontinuous solutions of the equations of hydrodynamics. *Matematicheskii Sbornik*, 89(3):271–306, 1959.
- G. Strang. On the construction and comparison of difference schemes. *SIAM Journal on Numerical Analysis*, 5(3): 506–517, 1968.
- G. I. Marchuk. On the theory of the splitting-up method. In *Numerical Solution of Partial Differential Equations-II*, pages 469 – 500. Academic Press, 1971.
- David L. Ropp, John N. Shadid, and Curtis C. Ober. Studies of the accuracy of time integration methods for reaction-diffusion equations. *J. Comput. Phys.*, 194(2):544–574, 2004. ISSN 0021-9991. doi:10.1016/j.jcp.2003.08.033. URL <https://doi-org.cyber.usask.ca/10.1016/j.jcp.2003.08.033>.
- A. J Christlieb, Y. Liu, and Z. Xu. High order operator splitting methods based on an integral deferred correction framework. *Journal of Computational Physics*, 294:224–242, 2015.
- Severiano González-Pinto, Domingo Hernández-Abreu, María S. Pérez-Rodríguez, Arash Sarshar, Steven Roberts, and Adrian Sandu. A unified formulation of splitting-based implicit time integration schemes. *J. Comput. Phys.*, 448: Paper No. 110766, 22, 2022. ISSN 0021-9991. doi:10.1016/j.jcp.2021.110766. URL <https://doi-org.cyber.usask.ca/10.1016/j.jcp.2021.110766>.
- Raymond L. Speth, William H. Green, Shev MacNamara, and Gilbert Strang. Balanced splitting and rebalanced splitting. *SIAM J. Numer. Anal.*, 51(6):3084–3105, 2013. ISSN 0036-1429. doi:10.1137/120878641. URL <https://doi-org.cyber.usask.ca/10.1137/120878641>.

- G. J. Cooper and A. Sayfy. Additive methods for the numerical solution of ordinary differential equations. *Math. Comp.*, 35(152):1159–1172, 1980. ISSN 0025-5718. doi:10.2307/2006380. URL <https://doi-org.cyber.usask.ca/10.2307/2006380>.
- A. Sandu and M. Günther. A generalized-structure approach to additive runge–kutta methods. *SIAM Journal on Numerical Analysis*, 53(1):17–42, 2015.
- E. Hairer, C. Lubich, and G. Wanner. *Geometric numerical integration: structure-preserving algorithms for ordinary differential equations*, volume 31. Springer Science & Business Media, 2006.
- C. A. Kennedy and M. H. Carpenter. Additive Runge–Kutta schemes for convection–diffusion–reaction equations. *Applied Numerical Mathematics*, 44(1-2):139–181, 2003.
- D. L. Ropp and J. N. Shadid. Stability of operator splitting methods for systems with indefinite operators: reaction–diffusion systems. *Journal of Computational Physics*, 203(2):449–466, 2005.
- D. L. Ropp and J. N. Shadid. Stability of operator splitting methods for systems with indefinite operators: Advection–diffusion–reaction systems. *Journal of Computational Physics*, 228(9):3508–3516, 2009.
- Saeed Torabi Ziaratgahi, Megan E. Marsh, Joakim Sundnes, and Raymond J. Spiteri. Stable time integration suppresses unphysical oscillations in the bidomain model. *Frontiers in Physics*, 2, 2014. ISSN 2296-424X. doi:10.3389/fphy.2014.00040. URL <https://www.frontiersin.org/article/10.3389/fphy.2014.00040>.
- Charles William Gear. Multirate methods for ordinary differential equations. Technical report, Department of Computer Science, Illinois University, Urbana (USA), 1974.
- Anne Kværnø. Stability of multirate Runge–Kutta schemes. *Int. J. Differ. Equ. Appl.*, 1A(1):97–105, 2000. ISSN 1311-2872. Tenth International Colloquium on Differential Equations (Plovdiv, 1999).
- Scott D. Cohen and Alan C. Hindmarsh. CVODE, a stiff/nonstiff ode solver in C. *Comput. Phys.*, 10(2):138–143, mar 1996. ISSN 0894-1866. doi:10.1063/1.4822377. URL <https://doi.org/10.1063/1.4822377>.
- G. Goldman and T. J. Kaper. Nth-order operator splitting schemes and nonreversible systems. *SIAM Journal on Numerical Analysis*, 33(1):349–367, 1996.
- A. T. Sornborger and E. D. Stewart. Higher-order methods for simulations on quantum computers. *Physical Review A*, 60(3):765–789, 1999.